

## Accurate wireless channel modeling for efficient adaptive Forward Error Correction in JPEG 2000 video streaming systems

<sup>1</sup>Max Agueh, <sup>2</sup>Magaye Diop,

<sup>1</sup>LACSC ECE, 37 Quai de Grenelle, 75725 Paris Cedex 15, France

<sup>2</sup>ESP, Université Cheikh Anta Diop, BP 5085 Dakar, Sénégal

---

**Abstract:-** In this paper, we evaluate the impact of accurate 802.11 based wireless channel modeling on the efficiency of dynamic Forward Error Correction (FEC) schemes in Motion JPEG 2000 video streaming systems. We derive a compromise on the suitable trace length for practical estimation of Packet Error Rate (PER) at decoder side. We demonstrate the validity of the derived trade-off using a real JPEG 2000 based video streaming system.

**Index Terms:-** Wireless channel modeling; trace length; analysis window length; dynamic Forward Error Correction; Packet Error Rate estimation; Motion JPEG 2000 video streaming.

---

### I. INTRODUCTION

With the development of wireless multimedia streaming systems there is an increasing demand on application level tools which could increase the robustness of video streaming over wireless networks. JPEG 2000 [1], the newest image representation standard, addresses this issue by predefining error resilient tools in its core encoding system (part 1) and going straightforward by defining in its 11th part called wireless JPEG2000 (JPWL) [2] a set of error resilient techniques to improve the transmission of JPEG2000 code streams over error-prone wireless channel. One of the main recommendations of JPWL final draft is the use of Forward Error Correction (FEC) with Reed-Solomon. Hence, in the literature, authors [3][4] proposed FEC rate allocation schemes for robust JPEG 2000 images and video streaming. These schemes statically [3] or dynamically [4] allocate JPEG 2000 code streams channel coding rate based on the estimation of respectively Bit Error Rate (BER) and Packet Error Rate (*PER*). In [4], at the decoder side, error rate metrics are derived after frame decoding and these metrics are used, at the encode side, to derive an application level channel model. The FEC rate allocation scheme relies on the derived channel model to select the appropriate channel codes for next frames protection. Hence, in wireless images and video streaming systems such as the one considered in this work (see Figure 1), the effectiveness of FEC rate allocation schemes depends on the accuracy of error rate estimation and channel modeling in the system.

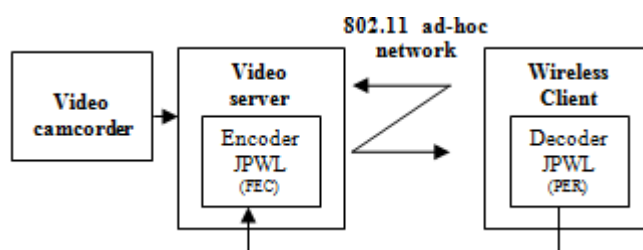


Figure 1. Wireless multimedia system

In this paper, we evaluate the impact of accurate Packet Error Rate (interchangeably Bit Error Rate) on the effectiveness of JPEG 2000 based FEC rate allocation schemes. Then, we define an analysis window length as the length of the used trace for *PER* estimation at decoder side. Ideally, the analysis window length should be the highest possible for accurate channel modeling, however due to the real time constraint this value must not be too high. By the other side, a very short analysis window length leads to bad channel modeling because the estimated *PER* is not statistically representative. Finally, we derive a trade-off point for practical estimation of analysis window length and we validate this compromise using an application of Motion JPEG 2000 video streaming over real ad-hoc networks traces.

To the best of our knowledge the present work is the first to give practical clues (compromise on analysis window length) for accurate wireless channel modeling in order to enhance the effectiveness of the FEC rate allocation schemes used in Wireless JPEG 2000 images and video streaming systems.

The paper is arranged as follows. Section II presents the two FEC rate allocation schemes considered in this work for robust JPEG 2000 images and video streaming over wireless networks. In section III, the loss patterns generation is described and an analysis of the considered real wireless channel traces is provided. A compromise on the suitable analysis window length for efficient FEC rate allocation schemes is also derived in section III. The results validating the derived empirical trade-off are presented in section IV. Finally, some conclusions are provided in section V.

## II. FEC RATE ALLOCATION SCHEMES

In this paper we considered two low-complexity Forward Error Correction schemes used respectively in [3] and [4] for robust JPEG 2000 based images/video streaming.

### A. Layered Unequal Error Protection Scheme

Z. Guo and al proposed in [3] a slightly complex layered unequal error protection scheme for robust Motion JPEG 2000 streaming over wireless network. This FEC rate allocation scheme relies on the contribution of each layer to the improvement of image quality to select the suitable RS codes. Hence powerful RS codes are set to most important layers such as the base layer and the other layers are protected by decreasing order of importance. However, this algorithm is not JPWL compliant and was designed based on the assumption that the channel is a memoryless Binary Symmetric Channel (uncorrelated error occurrence) which is not realistic because wireless channels have correlated errors sequences.

### B. Dynamic FEC rate allocation scheme

The second considered FEC rate allocation scheme is presented in [4] and is a dynamic layered based unequal error protection FEC rate allocation methodology for efficient JPEG 2000 streaming over MANET. This scheme is based on the assumption that transmitted JPEG 2000 image quality is linked to the amount of correctly decoded packets at the receiver. Hence, goal of this scheme is to maximize the overall throughput in the system. The dynamic FEC rate allocation scheme improves the performance by about 10% compared to a priori selection of channel coding.

The drawback of both methodologies is that their effectiveness depends on the accuracy of error rate estimation at decoder side. This paper addresses this issue by relying on real 802.11 traces analysis to derive a trade-off on the estimation window length for accurate Packet Error Rate evaluation.

In the following section we analyse the real MANET traces.

## III. APPLICATION LEVEL CHANNEL MODELING

### A. Loss Patterns Generation

The platform used to generate the loss patterns is presented in Figure 1. It consists of a client/server software pair running on two Windows XP laptops connected in ad-hoc network using two PCMCIA IEEE 802.11 b/g cards (at 2,4 GHz).



Figure 2. Loss patterns generation platform

The set of loss patterns generated covers different transmission scenarios (mobile or static). Each pattern corresponds to a specific Carrier to Noise ratio  $\frac{C}{N}$  ( $\frac{C}{N}$  is the ratio between the desired signal and the total received noise power). The used mode at the physical layer of the wireless link is the mode 4 where the modulation is QPSK, the coding rate is 3/4 and the Nominal Data Rate  $R_{Nominal}$  is 18Mbit/s. In the considered loss patterns,  $\frac{C}{N}$  varies between 20 dB and 11dB which corresponds to a Packet Error Rate ranging from

$5.1 * 10^{-3}$  to  $2.662 * 10^{-1}$ .

Generated traces are available in [5].

**B. Modeling Loss Patterns with Gilbert Model**

The Gilbert model was first introduced by Gilbert in [9]. Elliot proposes an extension of the Gilbert model in [10], the last model is commonly known as the Gilbert-Elliot (GE). In GE model, the wireless channel is modelled to have two states: good and bad. In the good state ( $g$ ), the channel provides a constant and low error probability ( $P_G$ ) whereas in the bad state ( $b$ ), the channel experiences a high error probability ( $P_B$ ). Hence we have  $P_G \ll P_B$  for GE, and  $P_G = 0$  and  $P_B = 1$  for the Gilbert channel, in other words the Gilbert model is a simplified GE model.

In this work, we consider an 8-bit symbol oriented model to emulate the correlated error characteristics of wireless channel. Therefore, our wireless channel is modelled as a two state Markov process (see figure 3). With this model, the channel produces error bursts.

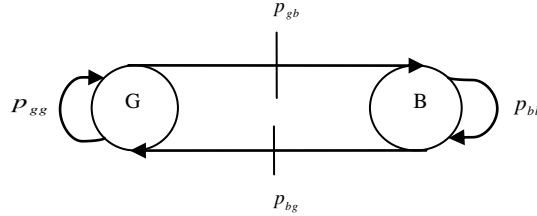


**Figure 3. Two state Markov process scheme**

Let  $L_G$  and  $L_B$  be respectively the mean length of error free and erroneous sequences, we have:

$$L_G = \frac{1}{1 - P_{gg}} \quad \text{and} \quad L_B = \frac{1}{1 - P_{bb}}$$

Applying Markov process at symbol level, we derive the Symbol Error Rate ( $SER$ ) for Gilbert model [9]:

$$SER = \frac{1 - P_{gg}}{1 - P_{bb} + 1 - P_{gg}}$$

A comprehensive description of the Markov modeling for wireless channel is explained in [11].

**C. Trace Analysis under Gilbert Framework**

It is worth noting that in the considered traces each packet had a fixed length of 1128 symbols (bytes). In our work we do not consider a cross layer estimation of transmission errors, so the Symbol Error Rate ( $SER$ ) is equal to the Packet Error Rate ( $PER$ ).

Therefore, packet oriented Gilbert models derived from traces had the same characteristics and same parameters than the 8-bit symbol oriented Gilbert models used to emulate the wireless channel at application level. As loss patterns are applied on packets, for coherence reason, a packet oriented analysis of the traces is presented.

In the loss patterns Good state (G) and bad state (B) are represented respectively by 0 and 1. Hence 0 corresponds to a well received packet and 1 to an erroneous packet. The distribution of error bursts is presented in figure 3-a for different loss patterns. From figure 3-a, it can be noticed that, in most cases, the error burst length is less than 10 packets. So  $L_B^{\max} = 10$  is considered as the upper bound of the error burst length.

The error free burst length distribution in figure 3-b shows that the upper bound  $L_G^{\max} = 100$  is ten times superior to the error bursts. This is due to the fact that apart from the moment when the wireless channel experience fading (bursts of errors), the transmission is often successful. We also notice that the number of error free bursts is lower than the number of error bursts, but this gap is compensated by the stay time in error free state (error free burst length) which is much longer than the one in error state (error burst length). So in the models used to emulate the traces, the mean time in the good state G should be sensibly greater than the mean time in the bad state B.

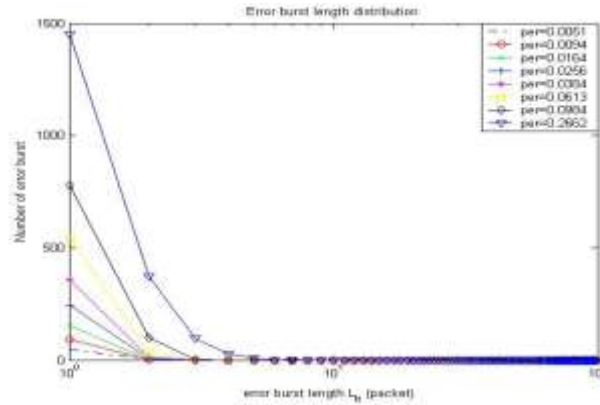


Figure 3-a. Error bursts distribution

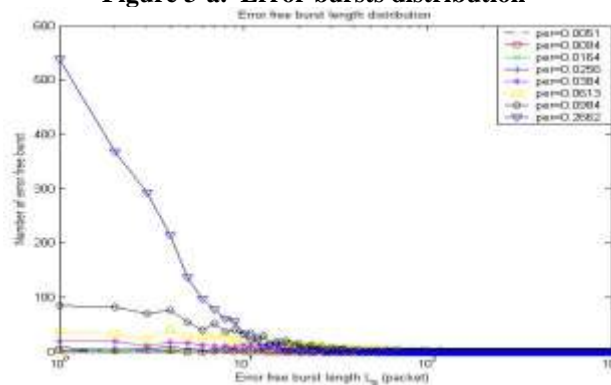


Figure 3-b. Error free bursts distribution

Figure 4-a presents the mean error burst length evolution for different traces. An exponential increase of the mean error burst length with the Packet Error Rate can be observed. It is worth noticing that even when the channel is highly noised, typically  $10^{-2} \leq PER \leq 10^{-1}$ , the mean error burst does not vary, and is about 1.05 packets. It can be deduced that our channel experiences relatively fast fading periods. In figure 4-b, the error burst length standard deviation is presented, in order to evaluate the fluctuation of the error burst length around the mean error burst length of the considered traces.

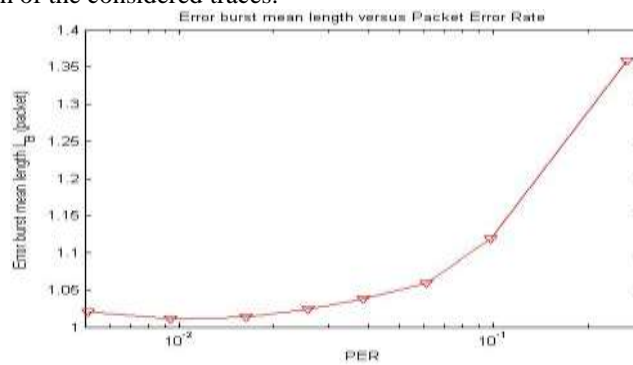


Figure 4-a. Error burst mean length versus PER

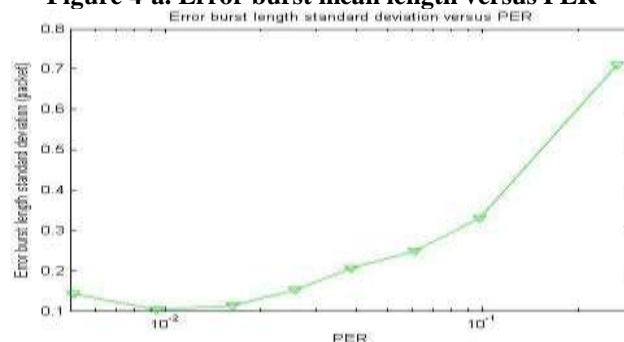


Figure 4-b. Error burst length standard deviation versus PER

Figure 4-b indicates that for slightly noised channel, typically  $10^{-2} \leq PER \leq 10^{-1}$ , the error burst length standard deviation is low, meaning that error burst length is closed to the mean value  $L_B$ , whereas for highly noised channel, typically  $PER \geq 10^{-1}$ , the error burst standard deviation is high, leading to a sensible fluctuation of error burst length around the mean value.

Similarly figure 5-a shows that the mean error free burst length decreases exponentially with the Packet Error Rate. Hence this metric varies between 100 and 200 packets for  $PER \leq 10^{-2}$ , and 100 and 10 packets for  $10^{-2} \leq PER \leq 10^{-1}$ .

For  $PER \geq 10^{-1}$  the mean error free burst length is 10 packets, which is ten times higher than the mean error burst length, demonstrating that even for highly noised channel the ratio between error free burst length and error burst length is still higher. It comes under view that the channel experiences longer error free sequence than error sequence which confirms the conclusions derived from figure 3-a and figure 3-b.

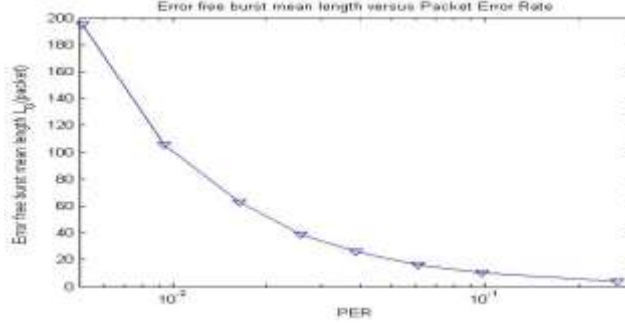


Figure 5-a. Error free burst mean length versus PER

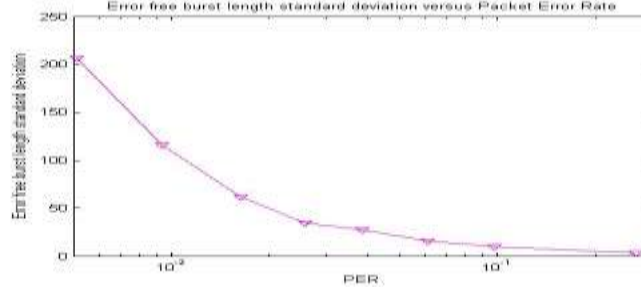


Figure 5-b. Error free burst length standard deviation versus PER

In figure 5-b the standard deviation of the error free burst length versus the Packet Error Rate is presented. We notice that for  $PER \leq 10^{-2}$ , error free burst length standard deviation is high meaning that error free burst length fluctuates a lot around the mean value  $L_G$  whereas for  $PER \geq 10^{-1}$  this metric is sensibly reduced making the error burst length closer to the mean value.

Thanks to loss patterns analysis, interesting information can be derived about the wireless channel such as the mean error free burst length  $L_G$  and the mean error burst length  $L_B$ . In previous section, we shown that,  $L_G$  and its associated standard deviation increase exponentially with  $PER$  whereas  $L_B$  and its associated standard deviation behave inversely. Those metrics are then used to derive the Gilbert model parameters  $p_{gb}$  and  $p_{bg}$  using the relation verified by R. Jain in [12]:  $p_{gb} = \frac{1}{L_G}$  and  $p_{bg} = \frac{1}{L_B}$ .

In our work each loss pattern had a fixed length of 10000 packets. Let evaluate, the impact of the considered traces length on the accuracy of its associated Gilbert model.

#### D. Impact of Analysis Window length on the Accuracy of Gilbert Models

In order to estimate the impact of the trace length on the accuracy of generated Gilbert models, the analysis window  $N$  and the parameters  $p_{gb}$  and  $p_{bg}$  are fixed. Then, a Monte-Carlo simulation is conducted using 1000 artificial traces of same length  $N$ . For each artificial trace, the parameters  $\hat{p}_{gb}$  and  $\hat{p}_{bg}$  are estimated.

Let  $\Delta p_{gb}$  and  $\Delta p_{bg}$  be the relative gap between the parameters estimated from artificial traces and from the

fixed Gilbert model parameters, we have:  $\Delta p_{gb} = \frac{|\hat{p}_{gb} - p_{gb}|}{p_{gb}}$  and  $\Delta p_{bg} = \frac{|\hat{p}_{bg} - p_{bg}|}{p_{bg}}$ . Let  $\sigma_{\Delta p_{gb}}^2$  and  $\sigma_{\Delta p_{bg}}^2$  be the variance respectively of  $\Delta p_{gb}$  and  $\Delta p_{bg}$ . The parameter  $\sigma_{\Delta p_{gb}}^2$  versus the analysis window length  $N$  is presented in figure 6-a.

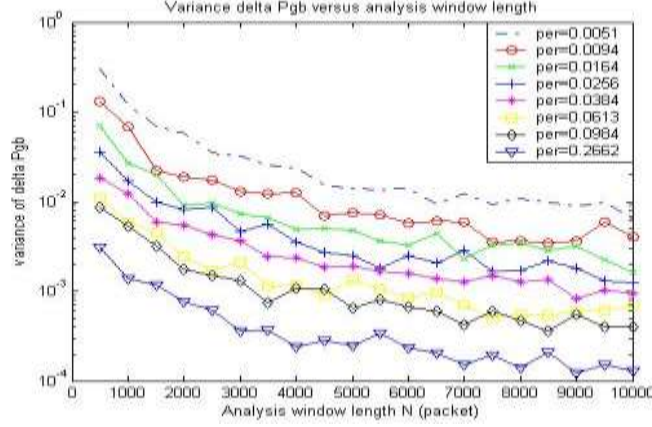


Figure 6-a. Variance of delta P\_gb versus analysis window length

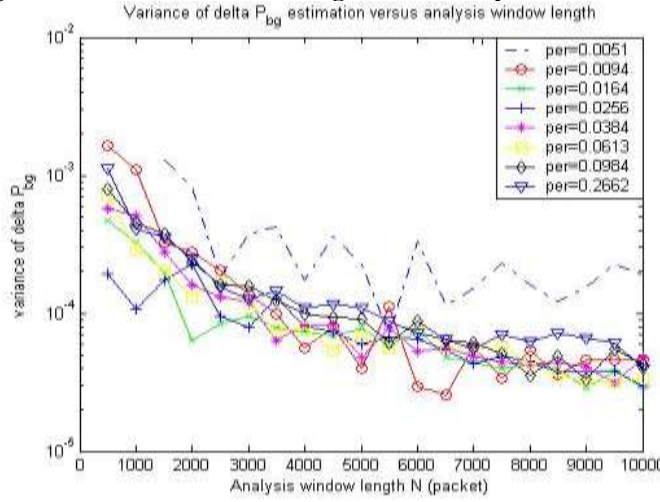


Figure 6-b. Variance of delta P\_bg versus analysis window length

We notice that increasing the analysis window length  $N$  decreases the variance of  $\Delta p_{gb}$  and so increases the accuracy on the estimation of the estimated  $p_{gb}$ . In other words, the more the trace length is long the more accurate is the estimated Gilbert model. This is due to the fact that the estimation of Gilbert parameter  $p_{gb}$ , relies on mean error free burst length whose value becomes statistically representative with the increase of the trace length. Moreover, we observe that increasing  $PER$  leads to a sensible reduction of the error made in the estimation of  $p_{gb}$ .

Indeed, for  $PER = 2.662 * 10^{-1}$  and with an analysis window of 1000 packets, we have  $\sigma_{\Delta p_{gb}}^2 = 1.5 * 10^{-2}$  whereas for the same  $N=1000$  and  $PER = 5.1 * 10^{-3}$  we have  $\sigma_{\Delta p_{gb}}^2$  close to  $10^{-1}$ . In the last case, the improvement in the accuracy of the model is about 60 times higher than in the previous case. Hence, the more the channel is erroneous, the more the estimation of  $p_{gb}$  is accurate. This is explained by the fact that increasing  $PER$  decreases the error free bursts length standard deviation as shown in figure 5-b. As the accuracy of  $p_{gb}$  is linked to statistically representative values of  $L_G$ , it comes under view that the considered parameter estimation changes with the  $PER$  whose sensitively impacts  $L_G$ . However, as shown in figure 6-b this is no longer the case for the estimation of parameter  $p_{bg}$ . From figure 6-b, it can be noticed that for analysis

window length of 1000, estimation of  $p_{bg}$  is slightly sensitive to  $PER$ , because we do not have enough error bursts to derive sufficiently representative measures of  $L_b$  in which we rely to estimate  $p_{bg}$ . However, as far as  $N$  significantly increases, we have a better estimate of  $p_{bg}$  and its estimation became less impacted by the  $PER$  increase for a considered analysis window length contrarily to  $p_{gb}$ . This is explained by the fact that increasing  $PER$  increases the number of error bursts but does not increase their length whose mean remains constant as shown in figure 4-a.

Finally, we can deduced from this section that for accurate Gilbert model parameters estimation, an analysis window length of at least 1000 packets (corresponding to 10% of the overall trace length) should be considered.

Going straightforward, we extend this trade-off to video streaming systems. Hence, denoting  $L_v$  as the video length, an interesting window length for accurate PER estimation is  $0.1 \times L_v$ . As an example, for a Motion JPEG 2000 video constituted by 200 frames, the PER at receiver should be estimated at least every twenty JPEG 2000 frames in order to guaranty the efficiency of the FEC rate allocation scheme. In the following section, we validate this empirical compromise using a Motion JPEG 2000 video streaming over real MANET traces.

#### IV. JPEG2000 VIDEO STREAMING RESULTS

The interest of this section is to validate the compromise on PER estimation window length in a real dynamic FEC rate allocation system.

The video sequence used is the *speedway.mj2* [13] containing 200 JPEG2000 frames at an overall quality of 0.2 bpp (bit per pixel) with 0.05 bpp for base layer, 0.1 bpp for the second layer and 0.2 bpp for the third layer.

As error occurrence in the transmission channel is a random process, different runs were made for each simulation and the Mean Square Error ( $MSE$ ) between the original image ( $I_o$ ) and the decoded image ( $I_d$ ), is averaged over all the runs in order to have statistically representative metrics.

The measured Peak Signal to Noise Ratio (PSNR) is obtained as follows:

$$MSE(I_o, I_d) = \frac{1}{M \cdot N} \sum_{x=1}^M \sum_{y=1}^N |I_o(x, y) - I_d(x, y)|^2$$

$$\overline{MSE} = \frac{MSE}{N_{frames}} \quad \text{and} \quad PSNR = 10 * \log_{10} \left( \frac{255^2}{\overline{MSE}} \right)$$

Where  $\overline{MSE}$  is the Mean Square Error over all the  $N_{frames}$  images considered. In the case of Motion JPEG2000 streaming,  $N_{frames}$  represents the 200 JPEG2000 frames constituting the video sequence Each PSNR measure is associated to a decoding rate metric which corresponds to crash estimation on the basis of frames transmission trials.

The FEC rate allocation schemes used are the one presented in section 2. Thanks to the wireless multimedia system presented in figure 1, the effectiveness of both data protection schemes is evaluated by computing the PSNR at the output of the system. Through a client/server application the JPEG2000 frames extracted from the Motion JPEG2000 (MJ2) file are transmitted to the receiver which represents the wireless client.

The Packet Error Rate is estimated at the decoder and sent back to the encoder via the uplink in order to improve next frames protection levels. Thanks to a better knowledge of the channel, the encoder selects a set of RS codes to protect each layer of JPEG 2000 frames.

In our work, the wireless channel is emulated using real loss patterns [5] presented in section 3. The considered loss patterns have  $\frac{C}{N} = 18 \text{ dB}$  and the Motion JPEG 2000 file (*speedway.mj2*) length is  $L_v = 8704 \text{ bytes}$ .

Figure 7 illustrates the selected  $RS(n, k)$  codes error correcting ability  $t = \frac{n-k}{2}$  versus the PER estimation window length while using the FEC rate allocation schemes presented respectively in [3] and [4]. Since the best set of selected RS codes are achieved with the maximal window length  $L_v$ , we notice that PER estimation (analysis) window length of  $0.1 \times L_v$  is enough to yield the suitable protection level for JPEG 2000 code streams. Using a PER estimation window length higher than the proposed trade-off leads to the same set of RS codes selection but decreases the reactivity of the system and by the way its effectiveness because PER values are

updated less frequently. On the over side, using a PER estimation window length lower than the proposed trade-off leads to inaccurate channel modeling which reduces the efficiency of the protection schemes.

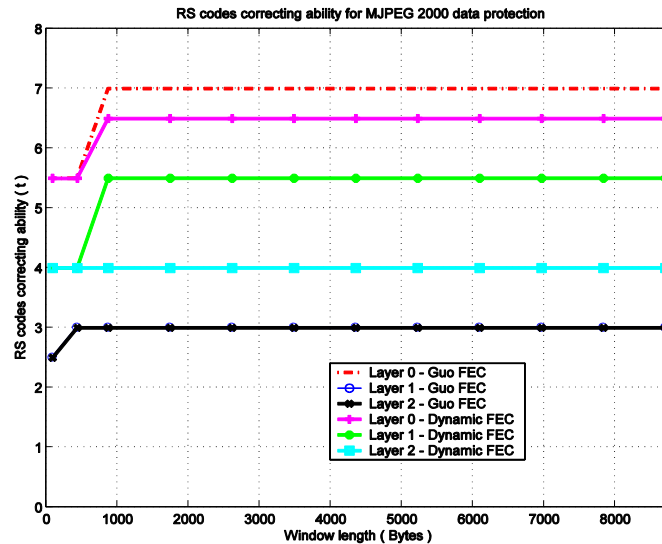


Figure 7. Correcting ability of the RS codes used for MJPEG 2000 data protection – Bandwidth 18 Mb/s. Table I and table II show the PSNR of decoded video sequence versus estimation window length while using the FEC rate allocation schemes presented respectively in [3] and [4].

TABLE I: PSNR OF VIDEO SEQUENCE AND IMAGES SUCCESSFUL DECODING RATE VERSUS PER ESTIMATION WINDOW LENGTH (Z. GUO)

Window length $L_V$ (bytes)	PSNR (dB)	Successful Decoding Rate (%)
$L_V$ (8704 bytes)	47.04	94
$0.1 \times L_V$ (871 bytes)	45.87	91
$0.01 \times L_V$ (88 bytes)	41.01	90

TABLE II: PSNR OF VIDEO SEQUENCE AND IMAGES SUCCESSFUL DECODING RATE VERSUS PER ESTIMATION WINDOW LENGTH (DYNAMIC FEC)

Window length $L_V$ (bytes)	PSNR (dB)	Successful Decoding Rate (%)
$L_V$ (8704 bytes)	47.12	94
$0.1 \times L_V$ (871 bytes)	46.02	93
$0.01 \times L_V$ (88 bytes)	41.22	91

We notice from table I and table II, that the PSNR of decoded video sequence is almost the same for PER estimation window length superior or equal to  $0.1 \times L_V$  ( $\approx 46$  dB). However, the PSNR decreases about 5 dB under the proposed trade-off point which implies a reduction of the video quality decoded by the wireless client. It is worth noting that the successful decoding rate is often higher than 90% which means that in our work even in case of inaccurate channel modeling, both FEC rate allocation schemes select sufficiently powerful RS codes to avoid decoder crashes.

We conclude that the proposed PER estimation window length is a valid trade-off for practical implementation of FEC rate allocation schemes in Motion JPEG 2000 video streaming systems. An interesting extension to this work could be the comparison of the results obtained using the proposed empirical window threshold to those achievable while using the sliding window algorithm proposed in [14].

## V. CONCLUSION

In this paper we evaluate the impact of the accuracy of the channel models on the effectiveness of application level FEC rate allocation schemes.

We start by presenting the considered FEC rate allocation schemes for robust Motion JPEG 2000 video streaming application over wireless channels. After analysing real 802.11 based traces we derived a compromise for the PER estimation window length at receiver side. The proposed estimation window length is about ten time less than the transmitted video length. We then show the validity of the proposed trade-off using an application of Motion JPEG 2000 video streaming of JPEG 2000 traces.

## REFERENCES

- [1]. D.S. Taubman et M.W. Marcellin, "JPEG 2000 Image Compression Fundamentals, Standards and Practice," Kluwer Academic Publishers, The Netherlands 2001
- [2]. JPEG 2000 part 11 Final Draft International Standard, ISO/IEC JTC 1/SC 29/WG 1 N3797
- [3]. Z. Guo, Y. Nishikawa, R. Y. Omaki, T. Onoye and I. Shirakawa, "A Low-Complexity FEC Assignment Scheme for Motion JPEG 2000 over Wireless Network", IEEE Transactions on Consumer Electronics, Vol. 52, Issue 1, Feb. 2006 Page(s): 81 – 86
- [4]. M. Agueh, J-F Diouris, M. Diop and F-O Devaux, "Dynamic channel coding for efficient Motion JPEG 2000 streaming over MANET," Proc. Mobimedia2007 conf, August 2007, Nafpaktos, Greece
- [5]. Loss patterns acquired during the WCAM Annecy 2004 measurement campaigns IST-2003-507204 WCAM, "Wireless Cameras and Audio-Visual Seamless Networking," project website: <http://www.ist-wcam.org>
- [6]. M. Agueh, J-F Diouris, "Application level channel modelling in wireless network: example of JPEG 2000 images/video streaming over wireless channel," In Proc. IRAMUS Workshop, Jan 2007, Val thorens, France
- [7]. Almudena Konrad, Ben Y. Zhao, Anthony D. Joseph, and Reiner Ludwig, "A Markov-Based Channel Model Algorithm for Wireless Network," Proc. International Workshop on Modeling, Analysis and Simulation of Wireless and Mobile Systems (MSWiM), 2001
- [8]. Ping Ji, B. Liu, D. Towsley, Zihui Ge, J. Kurose, "Modeling Frame-level Errors in GSM Wireless Channels," Internet performance symposium. V 55, issue 1-2 (Jan 2004)
- [9]. E. N. Gilbert, "Capacity of a burst noise channel," Bell Syst. Tech. J., vol. 398, pp. 1253-1266, Sept 1960
- [10]. O.Elliott, "Estimates of error rates for codes on burst-noise channel," Bell Syst.Tech. J., vol. 42, pp. 1977-1997, Sept 1963
- [11]. Julio Arauz, prashant Krishnamurthy, "Markov Modeling of 802.11 channels," In Vehicular Technology Conference, 2003.VTC 2003-Fall. 2003 IEEE 58<sup>th</sup>. Vol.2 , pp 771- 775, 6-9 Oct. 2003
- [12]. R. Jain, "The art of computer systems performance analysis," p 491- 1991
- [13]. Speedway video sequences have been generated by UCL. Available:<http://euterpe.tele.ucl.ac.be/WCAM/public/Speedway%20Sequence/>
- [14]. Z. Li, J. Chakareski, X. Niu, Y. Zhang and W. Gu, "Modeling and Analysis of Distortion caused by Markov-model burst packet losses in Video transmission," submitted to IEEE Trans. On Circuits and Systems for video Technology, 2008, Ref: LTS-article-2009-018. Available: <http://infoscience.epfl.ch/record/131189?ln=fr>